Mesoscale modeling of a complex coastal terrain in the South-Western Cape using a high horizontal grid resolution for viticultural applications

Valerie Bonnardot, Sylvie Cautenet

Mesoscale Atmospheric Modeling Using a High Horizontal Grid Resolution over a Complex Coastal Terrain and a Wine Region of South Africa

V. BONNARDOT*

Institute for Soil, Climate and Water of the Agricultural Research Council, Pretoria, South Africa

S. CAUTENET

Laboratoire de Météorologie Physique, UMR 6016-CNRS, Blaise Pascal University, Aubiere, France

(Manuscript received 1 February 2007, in final form 28 July 2008)

ABSTRACT

The Regional Atmospheric Modeling System (RAMS) was used to assess local air circulation patterns over the wine-producing Stellenbosch region of South Africa. Numerical simulations using four nested grids (25, 5, and 1 km, and 200 m of horizontal resolution) were performed for each day of February 2000 (during the grape-ripening period) over southern Western Cape Province. Modeled hourly data were extracted from the analysis files and used to produce mean hourly fields (temperature, relative humidity, wind speed, and radiation). Three runs with increasing horizontal resolutions for the finer grid were performed (run 1 with two nested grids of 25 and 5 km; run 2 with three nested grids of 25, 5, and 1 km; run 3 with four nested grids of 25, 5, and 1 km, and 200 m). For each event, the simulations of 1-km and 200-m resolution were superior to the 5-km-resolution simulation, especially in reproducing the local air circulations (sea and slopes breezes) because of a better representation of the local terrain (topography and vegetation cover). The use of a high-resolution grid (200 m) may be of greater value in the identification of potential terrain for viticulture.

1. Introduction

a. Viticulture in South Africa

South Africa is a young wine-producing country with an increasing area under vines (126 419 ha in 2006) and a production of 1.013 million gross liters (3.3% of the world production), which is eighth largest in terms of overall volume production. White varieties account for 55% (mainly Chenin Blanc, Colombard, Sauvignon Blanc, and Chardonnay) and red varieties for 45% (mainly Cabernet Sauvignon, Shiraz, Merlot, and Pinotage) of the total area. Locally, viticulture represents 8.2% of the gross product of the Western Cape Province and there are 257 000 persons working directly or indirectly in the wine industry (SAWIS 2006). It, therefore, forms one of the vital economic sectors of the province. To remain competitive in an ever-expanding international wine market, the South African wine industry considers the "*terroir*" identification for viticulture of high priority and fosters research on this topic. This falls in line with the research identified by the Office International de la Vigne et du Vin (information online at http://www.oiv.org/presentation/oiv_uk.htm). Terroir is the interaction among climate, geology, soil, and topography (Falcetti 1994). Climate, one of the terroir components, plays a great role in determining wine character and quality differences. Temperature is accepted as being the parameter having the greatest effect on the physiology of the grapevine and specific reactions that occur during berry maturation (Jackson 2000) and, thus, final berry composition. This has been proven in South Africa with a number of studies on the effects of microclimate on wine character, especially on the Sauvignon Blanc cultivar (Marais 1994; Conradie et al. 2002). It was shown for instance that cool conditions favored the development of grape aromas, especially for white cultivars, for example, a high concentration of methoxypyrazines responsible for the typical green pepper and

* Current affiliation: Bureau d'Études et de Recherches en Climatologie Appliquée à la Vigne, Cranves-Sales, France.

Corresponding author address: Prof. Sylvie Cautenet, Laboratoire de Météorologie Physique, Blaise Pascal University, 24, Av. des Landais, Aubiere 63170, France.
E-mail: s.cautenet@opgc.univ-bpclermont.fr

DOI: 10.1175/2008JAMC1710.1

grassy aroma in Sauvignon Blanc (Marais et al. 1999). The mesoclimate has been investigated in application to viticulture in the traditional wine-producing area of the south Western Cape (Le Roux 1974) or in the whole Western Cape Province (De Villiers et al. 1996; De Villiers 1997). There have been a large number of climate-related studies within various wine-producing districts (Bonnardot 1999, 2002; Carey 2001; Bonnardot et al. 2001, 2002; Carey et al. 2002; Hunter and Bonnardot 2002; Conradie et al. 2002).

b. Location and climate of the study domain

The south Western Cape region occupies the most southwestern part of South Africa. The country is situated at the southern tip of Africa roughly between the latitudes of 22° and 35°S within the high pressure belt (centered on 30°S approximately) and skirted by the circumpolar westerly airstream to the south. It is thus almost entirely under the influence of the westerly circulation, especially in winter when the high pressure system moves 3°–4° farther north. At the surface, the weather is characterized by a succession of cyclones and anticyclones moving eastward across the country. In summer, an equatorial low pressure trough lies over the interior of the continent. The mean atmospheric circulation and the different synoptic weather patterns over southern Africa are explained in detail in Preston-White and Tyson (1988) and the large-scale factors influencing the climate of South Africa are provided in the general survey on the climate of South Africa (Schulze 1994). The extreme south Western Cape, our study domain, where the traditional vineyards lie, experience a *Mediterranean* type of climate (nontropical winter rainfall, warm and dry summers), which is a temperate climate characterized by pronounced summer droughts. It is under the influence of maritime air masses, which moderate diurnal temperatures, preventing excessively high temperatures during summer or excessively low temperatures during winter. This Mediterranean type of climate abuts the coastal fringes and progressively grades into semiarid conditions inland. The rest of the country passes progressively under a subtropical influence (aridity and summer rainfall of tropical origin). Along the coast, the increase in temperature northward is smaller than the increase inland per unit distance. The extreme south Western Cape receives the bulk of its rainfall (600–900 mm) from late autumn to the beginning of spring (80% between April and September). Summer is warm to hot, but not excessively so (maximum February temperatures are below 29°C), and dry, similar to areas in the Mediterranean region. Winter is cool, with a mean temperature above 10°C, and frost rarely occurs.

It is also flanked by the Atlantic Ocean with the cold Benguela Current to the west and the Indian Ocean with the warm Mozambique and Agulhas Currents to the east. The topography of the study domain is characterized by indented complex coastlines (the cape peninsula to the extreme southwest, Table Bay to the west, and False Bay to the south) associated with a mountainous inland terrain, with relatively high ranges, valleys, and plains (Fig. 1). The coastal plain is indented by hills (Tygerberg, 457 m; Bottelaryberg, 476 m) and is bordered by the NW–SE mountain ranges of Helderberg (1137 m) and Simonsberg (1390 m). As a result, there are large variations in the aspects and altitudes, as well as a sea–land temperature difference, which generate local air circulations (land and sea breezes and up- and downslope breezes). As a result of the combined effects of the proximity of the ocean and the complexity of the topography, significant temperature differences occur over very short distances in the wine region (Bonnardot 1999; Bonnardot et al. 2001, 2002; Carey 2001; Conradie et al. 2002; Hunter and Bonnardot 2002).

c. Mesoscale air circulation and sea-breeze investigations in the study domain

Mesoscale air circulations have been studied extensively in many regions of the world, initially using surface and upper-air observations, then by using early linear analytic models, and, more recently, complex nonhydrostatic numerical models for weather forecasting and air pollutant transport assessment. Numerical simulations of sea breezes have been performed to study their impacts on the economy, farming, the environment, or health interests, especially in increasingly populated coastal regions. Abbs and Physick (1992) and Miller et al. (2003) presented well-documented overviews of this phenomenon, showing its characteristics, its behavior in complex terrain, and its impacts. In South Africa, sea breezes have been studied particularly in the wine-producing Stellenbosch region due to the relevant climatic implications on grapevine performance and wine characteristics. The associated increase in wind velocity in the afternoon and concomitant increase in relative humidity and reduction in temperature (Planchon et al. 2000; Bonnardot 2002; Bonnardot et al. 2001, 2002, 2005) were of particular interest for the wine industry because of the significant effects of temperature (Kliewer and Torres 1972; Coombe 1987), relative humidity (Düring 1976; Champagnol 1984; Gladstones 1992), and wind (Freeman et al. 1982; Campbell-Clause 1988; Hamilton 1989) on grapevine physiology and thus potentially on the character of the resultant wine (Marais et al. 1999). The interactions between climatic

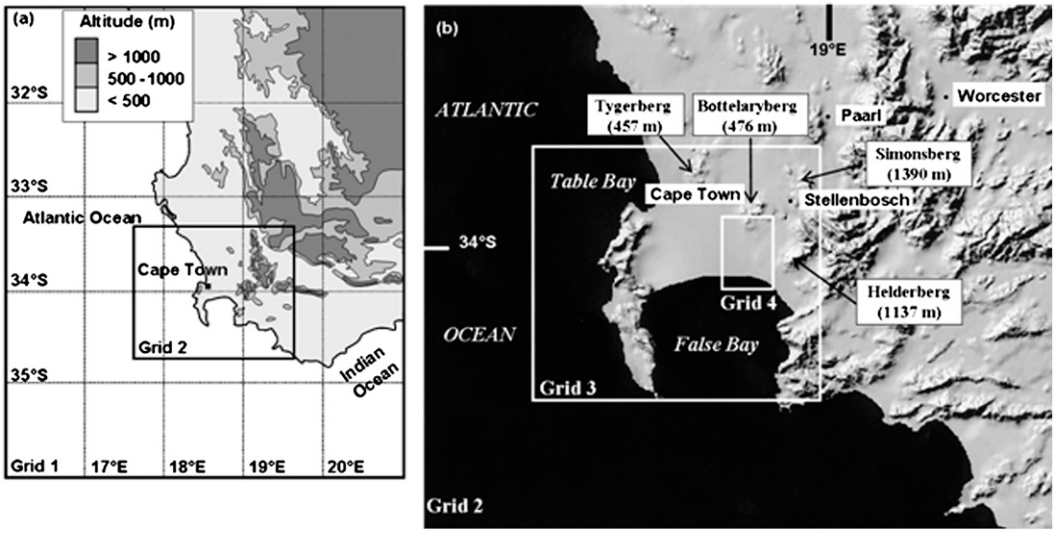

FIG. 1. Model area, complex topography, and nested grids, (a) grids 1 and 2 and (b) grids 2–4, for simulations over the extreme southwestern Cape of Good Hope.

parameters and grape performance and wine quality and character have been compiled by other authors (Champagnol 1984; Huglin and Schneider 1998) and summarized (Carey et al. 2002). The climatic requirements for the optimum physiological performance of the vine are between 25° and 30°C for temperature (Kriedemann 1968), between 60% and 70% for relative humidity (Champagnol 1984) and less than 3–4 m s^{-1} for wind speed (Freeman et al. 1982; Hamilton 1989). Temperature, relative humidity, and wind were therefore studied. In addition, recorded observations were available from a network of automatic weather stations located in or in proximity to vineyards. Sunshine duration, solar radiation, and light intensity, also important factors for vine physiology, as well as other relevant weather elements were not included in this study because of a lack of data recorded in the vineyards that could be compared with results from our sea-breeze simulations.

Sea-breeze studies were initiated (Bonnardot 1999) using surface data from the Agricultural Research Council's (ARC) automatic weather station network situated in the vineyards of the Stellenbosch wine district for the month of February over 3 yr (1996–98) in order to investigate the extent and climatic influences of the sea-breeze circulation in the wine region during the ripening period of most cultivars. During summertime, there was a significant contrast between the cool ocean associated with the cold Benguela Current (below 15°C in some places) and the high inland temperatures (mean February temperature was 22°C at Cape Town airport), resulting in a frequent occurrence of the sea breeze. The sea-breeze circulation was a daily phenomenon during the warm south Western Cape summer. The frequency analysis of the surface winds in the Stellenbosch wine district revealed that 30%–64% of the wind directions, depending on the locations, were from the sea, especially in the afternoon. There was also a sudden change in direction from predominantly north and northeast (land breeze) at night to predominantly west and southwest (sea breeze) in the afternoon, accompanied by an increase in wind velocity [mean maximum wind velocity of 5 m s^{-1} at 1700 South African standard time (SAST)]. However, modeling soon appeared necessary and was undertaken using the Regional Atmospheric Modeling System (RAMS). The first numerical simulations performed over the wine-producing Stellenbosch area used two nested grids (25- and 5-km resolution) for 2 days under onshore synoptic wind conditions (3–4 February 2000) (Planchon et al. 2000; Bonnardot et al. 2001). The sea-breeze circulation combined with the southern large-scale flow and, at the maximum stage of its development (1700 SAST), the modeled results for the 5-km grid resolution showed that the penetration of the sea breeze resulted in lower temperatures (<25°C) closer to the coast and that the optimum temperature requirements for grapevine photosynthesis (25°–30°C) in Kriedemann (1968) were met in a region located between approximately 15 and 35 km from False Bay. These results were similar to the observed data in the vineyards.

To ascertain the contributing effects of topography and synoptic flow on the local circulation and to help in understanding the climatic implications over the Stellenbosch vineyards, a third grid using an increased resolution (1 km) was added and simulations were performed using RAMS for different days under various synoptic conditions during the grape maturation period

(February). A southerly large-scale flow associated with warm conditions (3 February 2000), a northerly large-scale flow associated with hot and dry conditions from the interior (18 February 2000), and a northwesterly large-scale flow associated with cool and humid conditions (19 February 2000) were considered (Bonnardot 2002). The higher the inland temperature is, the greater is the temperature decrease induced by the sea breeze, and, depending on the direction of the large-scale flow in the boundary layer, the sea-breeze circulation was strengthened, deviated, or even prevented from penetrating inland. A description of the situations with southerly and northerly synoptic winds is given in Bonnardot et al. (2002, 2005), respectively. In the first case, it was shown that the sea breeze was a thin layer (50–100 m) with high humidity (>80%) above False Bay that penetrated up to 5 km inland with the sea-breeze development up to the southern slopes of the first hill and, depending on topography, a relative humidity of 50% was recorded between 10 and 15 km inland (Bonnardot et al. 2002). In the case with a northerly large-scale flow, it was shown that a sea breeze developed first at 1400 SAST from the Atlantic Ocean and Table Bay under onshore conditions. It was a 400-m-thick layer with a relative humidity above 65%, which penetrated up to 15 km eastward. At the same time, a shallow (100 m) sea breeze developed over False Bay, but remained out at sea, opposing the northerly synoptic wind. Then later, at 1700 SAST, the sea breeze that had originated from False Bay under offshore conditions thickened (400 m with humidity $> 60\%$) and penetrated inland up to 10 km from the coast, converging with the one from Table Bay over the Stellenbosch wine-producing region. The associated increase in wind velocity (>8 m s^{-1}) may have had a negative impact on grapevine physiology, but the temperature reduction, as much as 6°C at some locations, may have reduced the duration and the intensity of thermal stress experienced by the grapevines under the warm conditions (Bonnardot et al. 2005).

d. Justification for using a 200-m high-resolution grid

Because the choice of sites for viticulture depends on natural factors (soil and climate particularly), numerical simulations over the wine-producing area using a high horizontal grid resolution (i.e., less than 1 km), were necessary in order to assess the local circulations in greater detail. The modeling outputs help in identifying locations based on their potential to meet climatic requirements for optimum physiological performance of the vine and, therefore, facilitate recommendations for terroir election and zoning. Within the framework of mesoscale circulations, many numerical studies have investigated the best horizontal resolution that can be used. It is clear that for local circulations forced by topography and surface contrasts, increasing the resolution is desirable. McQueen et al. (1995) found that a 2.5-km grid in combination with high vertical resolution produced more realistic structures than those predicted by a 10-km grid. Rao et al. (1999) used two-way interactive domains with 1.4-, 0.4-, and 0.1-km horizontal grid spacings to show that less than 1-km grid spacing was required to realistically simulate the diurnal circulations of the Cape Canaveral region of Florida. However, Mass et al. (2002), sifting through 2 yr of results, showed that decreasing grid spacing in mesoscale models to less than 10–15 km generally improved the realism of the results but did not necessarily significantly improve the objectively scored accuracy of the forecasts. Colby (2004) indicated in the analysis of individual cases that the high-resolution grid (4 km) was able to resolve realistic details in the flow, details that coarse grids (34 or 40 km) missed entirely, but that the ability to forecast specific variables (like surface dewpoint) at specific locations was not improved by using a higher-resolution grid.

The high horizontal resolution, chosen to pursue the sea-breeze studies over the Stellenbosch wine district, is a 200-m grid in order to discriminate between areas with the potential to promote viticulture (Du Preez 2006). That paper contains an explanation of the modeling configurations on different days where sea-breeze circulations developed under different meteorological conditions, and a comparison is made between the numerical results and the observed data from four automatic weather stations located in the Stellenbosch wine district. Results from the 200-m grid resolution for temperature, relative humidity, wind speed, radiation, and vapor pressure were compared with those of the 1- and 5-km grid resolutions.

2. Atmospheric modeling using a high-resolution grid (200 m)

Version 4.3 of RAMS (information online at http://www.atmet.com) is a meteorological model developed for the simulation and forecasting of weather systems (Cotton et al. 2003). RAMS is primarily a limited-area model, and many of its parameterizations have been designed for mesoscale or higher-resolution scale grids. The model includes nested grids. The two-way exchange of information between the domains uses Clark's algorithms described in Clark and Farley (1984) and Walko et al. (1995). The atmospheric model is constructed around a full set of nonhydrostatic, compressible equations that describe the atmospheric dynamics and thermodynamics, plus conservation equations for scalar quantities such as

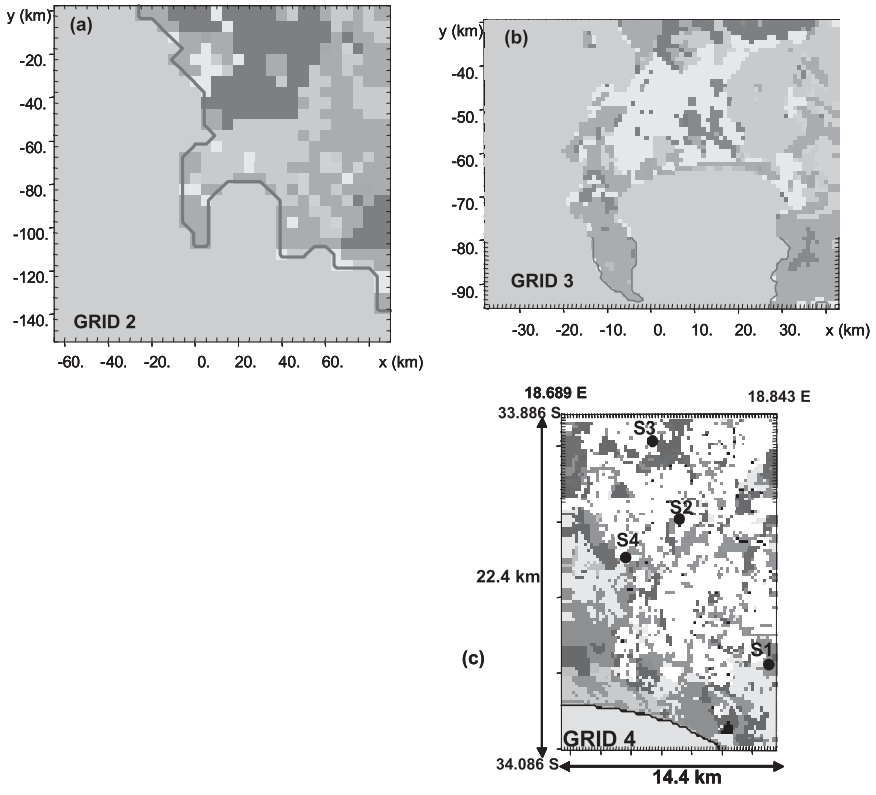

FIG. 2. Land cover for (a) grid 2 (5-km resolution), (b) grid 3 (1-km resolution), and (c) grid 4 (200-m resolution). White color represents vineyards. Automatic weather stations are black spots in grid 4.

water vapor and liquid and ice hydrometeor mixing ratios. These equations are supplemented with a large selection of parameterizations for turbulent diffusion; solar and terrestrial radiation; moist processes, including the formation and interaction of clouds and precipitating liquid and ice hydrometeors; kinematic effects of terrain; cumulus convection; and sensible and latent heat exchanges between the atmosphere and surface, consisting of multiple soil layers, vegetation, snow cover, canopy air, and surface water. A review of the role of land surface models in atmospheric models, including version 2 of the Land Ecosystem–Atmosphere Feedback (LEAF-2) in RAMS is given in Chen et al. (2001). RAMS has been used in a variety of studies to demonstrate the role of landscape variability in the generation of mesoscale wind flow.

Numerical simulation

A two-way interactive nested grid configuration with four grids was used, with each grid covering a different domain size (Figs. 1a and 1b). Grid 1 covered a domain between 31°00′ and 36°00′S and 16°00′ and 21°00′E (550 km × 475 km), which is the extreme southwestern region of South Africa as well as part of the South Atlantic Ocean and the Indian Ocean. With a horizontal resolution of 25 km, the coarse grid was principally devoted to synoptic circulations. Grid 2 (33°15′–34°45′S and 17°40′–19°30′E) represented an intermediate scale with a horizontal resolution of 5 km. Grid 3 (33°43′–34°23′S and 18°08′–18°57′E), with a horizontal resolution of 1 km, was the investigated domain for the local circulations (sea-breeze simulations) study. It had a 67 km × 82 km horizontal dimension. Finally, grid 4 (33°54′–34°06′S and 18°42′–18°51′E), with a high resolution of 200 m, covered a restricted domain over vineyards situated southwest of Stellenbosch (22.4 km × 14.4 km) (Fig. 2c). A 10-s time step as well as 30 levels in the vertical dimension (the same as in the four grids) and 15 levels from the surface to 1500 m were used, ensuring a fine description of the boundary layer.

Meteorological fields from the European Centre for Medium-Range Weather Forecasts (ECMWF) database initialized the domain and were nudged every 6 h at the lateral limit of grid 1. Local sea surface temperatures (SSTs) measured along the coast of the south Western Cape and supplied by the South African Weather Service (SAWS) were added to those obtained from the ECMWF, derived from Meteosat satellite, in

TABLE 1. Attributes of the four automatic weather stations used in the study and located in the Stellenbosch wine of origin district.

Name (reference)	Lat (°S)	Lon (°E)	Distance from False Bay (km)
Alto (S1)	34.01413	18.8559	8
Bonfoi (S2)	33.93527	18.78041	12.2
Goedehoop (S3)	33.91529	18.75904	17
Jacobsdal (S4)	33.96616	18.72837	9.7

order to account for the large variation in local SST. Topographical data were obtained from the National Oceanic and Atmospheric Administration (NOAA) at 30-s resolution for the first three grids. For grid 4, the topography was obtained from the Institute for Soil, Climate and Water (ISCW) and the Infruitec-Nietvoorbij Institute for Deciduous Fruit, Vines and Wine (of the Agricultural Research Council) elevation maps of the region. A land-use data file, at 200-m grid resolution, was aggregated to the resolution of each grid and adjusted to the 30 land cover classes used by RAMS. These classes were mostly characterized by vegetation type or whether the surface was covered with water, had bare ground, or was urban. Each of these classes was assigned a set of land surface parameter values including leaf area index, vegetation fractional cover, vegetation height, albedo, and root depth. The vegetation cover patterns for grids 2–4 are displayed in Figs. 2a–c, respectively. Grid 4 exhibits heterogeneous land cover in which vineyards dominate. A total of 12 soil texture classes were also parameterized in RAMS, and soil texture files for each grid were built (data from the Land Type Survey Staff 1995). Soil moisture was obtained from ECMWF.

3. Observed surface data for the studied episodes

February is the ripening period for most wine grapes in the Western Cape Province of South Africa. It is the warmest month of the year and, in the south Western Cape region, it is the period during which the sea–land temperature difference is at a maximum, which results in frequent sea-breeze circulations. To compare the numerical results with observations, three meteorologically contrasting 2-day episodes during the month of February 2000 were examined using hourly data from four automatic weather stations from the ARC Infruitec-Nietvoorbij network located in the vicinity of vineyards within grid 4 (Fig. 2c, Table 1). Temperature, relative humidity, and wind speed and direction at 2 m AGL were analyzed.

Values of maxima or minima, depending of the meteorological parameters, as well as of the monthly means for February 2000, are given in Table 2. Compared to a 30-yr-long term average (1971–2000) using surface data from the Nietvoorbij mechanical weather station of the ARC, February 2000 was warmer than average. Mean minimum and maximum temperatures for February 2000 were 15.9° and 28.8°C, respectively, which is 0.5° and 0.6°C above the 30-yr average (15.4° and 28.2°C respectively). The February 2000 minimum relative humidity (31%) was below average (39%).

TABLE 2. Minimum, maximum, or mean values for temperature, wind speed, and relative humidity (February 2000) at four surface weather stations (S) located in the Stellenbosch wine of origin district.

Meteorological parameters		Locations: Alto (S1)	Bonfoi (S2)	Goedehoop (S3)	Jacobsdal (S4)
Temperature (°C)	Max	38.09	38.24	36.25	36.23
	Mean	22.98	22.07	21.23	20.96
Wind speed ($m\ s^{-1}$)	Max	7.0	9.0	9.62	7.33
	Mean	2.0	3.39	3.78	3.40
Relative humidity (%)	Min	27.8	40.9	33.3	32.5
	Mean	72.47	78.4	75.19	73.15

The observed extreme maximum temperatures for February 2000 reached values between 36° and 38°C, while mean temperatures were between 21° and 23°C. The maximum wind speed at 2 m AGL reached values between 7 and 9 m s^{-1}, while the mean wind speed was between 2 and 4 m s^{-1}. The extreme minimum relative humidity ranged between 21% and 23% and the mean relative humidity was 75%. The temperature, wind speed, and relative humidity variations during the 2-day episodes at S1 (Alto), S2 (Bonfoi), S3 (Goedehoop), and S4 (Jacobsdal) are displayed as solid lines in Figs. 3–5. Although these stations are about 5–10 km apart, significant differences did occur over short distances (Table 2, Figs. 3–5). The adjectives ''high'' and ''strong'' used thereafter to describe the temperature and wind conditions in the vineyards were defined according to the temperature and wind thresholds for maximum grapevine photosynthesis (i.e., temperatures higher than 30°–35°C and wind speeds faster than 3–4 m s^{-1} can be considered to be stressful conditions for grapevines).

a. 3–4 February 2000

During this event, the dominant southerly flow (sea origin) was weak (4–5 m s^{-1}) on 3 February, but strengthened on 4 February, reaching a velocity of 6–7 m s^{-1}. On 3 February, maximum temperatures reached 28°–33°C over the Stellenbosch wine district and were associated with relative humidity values of 45%–60%, while on 4 February, maximum temperatures were lower (24°–26°C) and relative humidities higher (70%–80%). These weather conditions favor optimal physiological

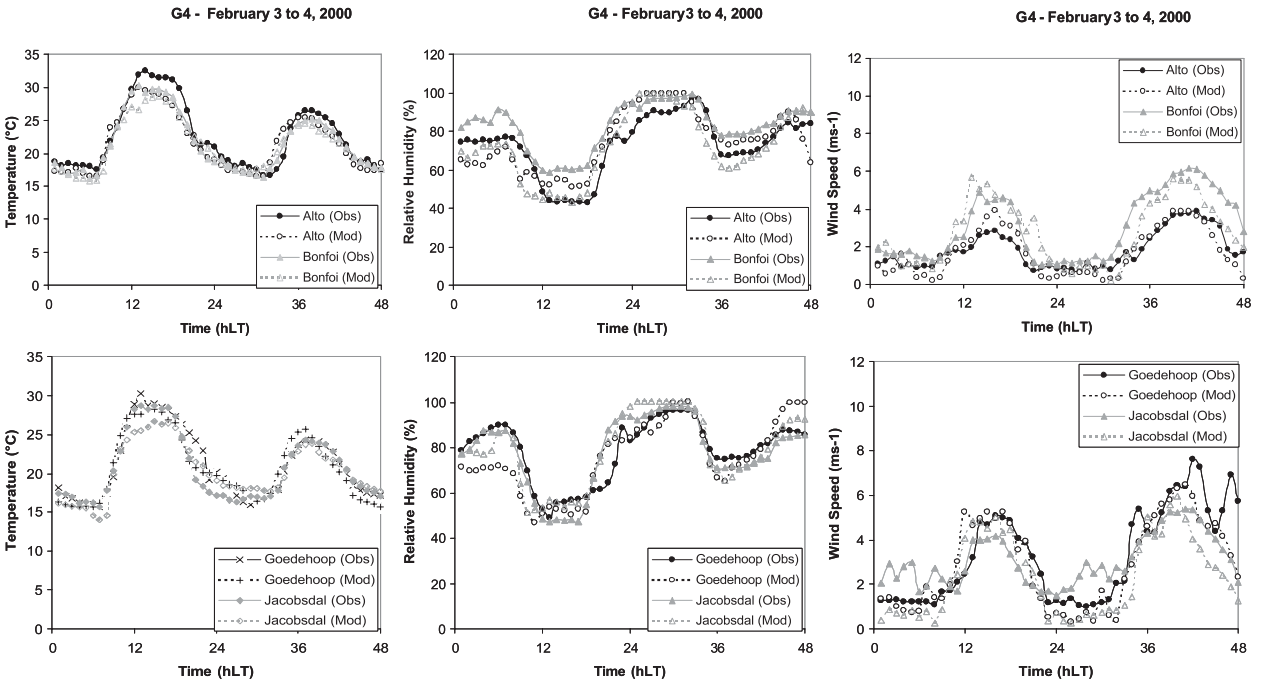

FIG. 3. Observed (solid lines) and modeled (dotted lines) data for temperature, wind speed, and relative humidity at 2 m AGL on 3–4 Feb 2000. Modeled data are extracted from run 3 using four grids.

functioning of the grapevines, although the wind velocity (above 4 m s^{-1}) may have inhibited photosynthesis.

Previous studies (Planchon et al. 2000; Bonnardot et al. 2002) showed strong sea-breeze development over the region during this period.

b. 12–13 February 2000

The meteorological conditions were characterized by a strong (for viticulture) southerly flow, which enhanced the sea-breeze circulation. On 12 February, the maximum

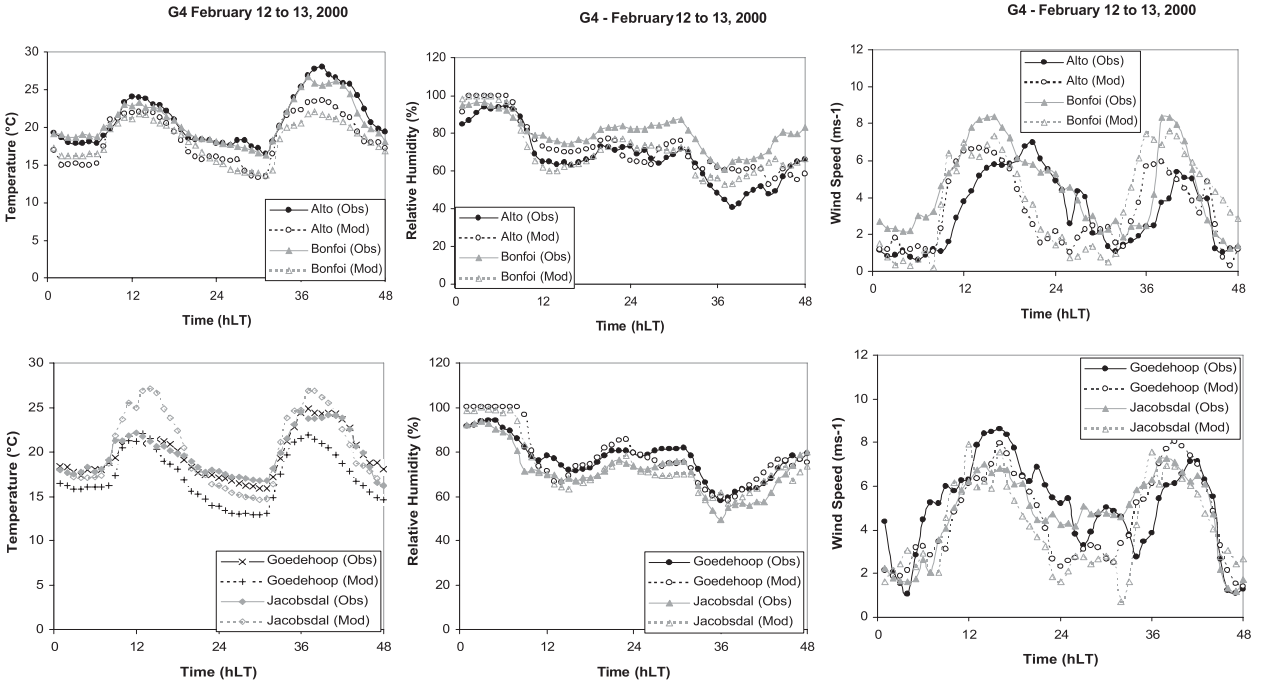

FIG. 4. As in Fig. 3, but for 12–13 Feb 2000.

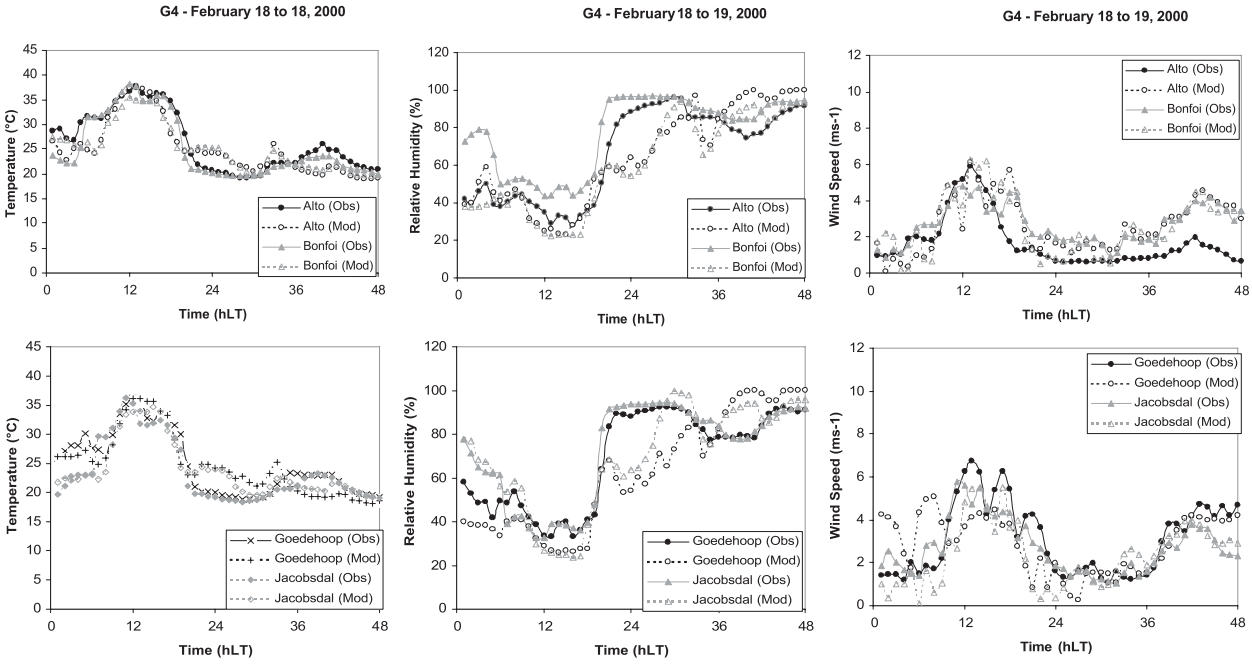

FIG. 5. As in Fig. 3, but for 18–19 Feb 2000.

temperatures were 21°–24°C, associated with humidity values above 60% and strong winds of 7–8 m s^{-1}, that is, above the recognized 4 m s^{-1} threshold, which resulted in increased stomatal resistance (Campbell-Clause 1988). On the following day, 13 February, the sea breeze was well developed with a wind velocity of around 5–8 m s^{-1}, maximum temperatures between 24° and 28°C [close to the optimum temperature requirements for grapevine photosynthesis: 25°–30°C in Kriedemann (1968)], and relative humidity between 40% and 60%.

c. 18–19 February 2000

The synoptic conditions were characterized by an intense high pressure system over the interior of the southwestern part of South Africa, and a low pressure system (coastal low) along the west coast of South Africa, which produced a warm offshore airflow (Berg winds) ahead of the trough system (on 18 February 2000) and cooler onshore airflow behind it (on 19 February 2000), as it moved toward the south and the southeast (Bonnardot et al. 2005). As a result, on 18 February, a strong (6–7 m s^{-1}) dominant wind from north imposed high temperatures (37°–38°C at 1400 SAST) over the vineyards accompanied by low relative humidity values (30%), that is, very high and dry conditions for the vines, while, on 19 February, the Stellenbosch region was characterized by lower temperatures (23°–26°C at 1400 SAST), very high humidity (100%), and weak winds (3–4 m s^{-1}), which were less stressful weather conditions for the vines.

4. Comparison between numerical results and observations according to the different resolutions used

Three runs using different horizontal resolutions were performed. Run 1 using a coarse resolution (5 km) was composed of two nested grids (grids 1 and 2), run 2 using a fine resolution (1 km) of three nested grids (grids 1–3), and run 3 using a high resolution (200 m) for four nested grids (grids 1–4). For each run, the numerical results were compared to the observations from the four surface automatic weather stations (S1–S4) situated in the Stellenbosch region (Fig. 2c). To estimate the errors between the simulated and observed values, the root-mean-square error (RMSE) and the relative error (RE) for each one of three contrasting events (3–4, 12–13, and 18–19 February) were calculated for every hour and for each station and each run (Table 3) as follows:

$$\mathrm{RMSE} = \left[N^{-1}\sum_{i=1}^{N}(P_i - O_i)^2\right]^{0.5} \quad \text{and}$$

$$\mathrm{RE} = (\mathrm{RMSE}/\overline{O}),$$

where O_i and P_i are the observations and the modeled values, respectively, at the hour i; N is the number of cases, equal to 48 (48 h for 2 days); and $\overline{O}$ is the mean of

TABLE 3. RMSE and RE (set in italics) for three studied events (2-day mean) for runs 1–3, for the parameters of temperature, wind speed, and relative humidity, at the four weather stations located in the Stellenbosch wine of origin district.

	Temperature (°C)											
	Alto (S1)			Bonfoi (S2)			Goedehoop (S3)			Jacobsdal (S4)		
Events	Run 1 (G2)	Run 2 (G3)	Run 3 (G4)	Run 1 (G2)	Run 2 (G3)	Run 3 (G4)	Run 1 (G2)	Run 2 (G3)	Run 3 (G4)	Run 1 (G2)	Run 2 (G3)	Run 3 (G4)
3–4 Feb 2000	3.44 *0.153*	2.19 *0.097*	1.95 *0.087*	1.21 0.056	1.68 *0.078*	1.13 *0.057*	4.26 *0.202*	2.90 *0.138*	1.46 *0.070*	1.72 *0.083*	1.43 *0.070*	1.49 *0.072*
12–13 Feb 2000	2.37 *0.112*	2.53 *0.120*	2.77 *0.132*	2.53 *0.122*	2.61 *0.126*	2.74 *0.132*	2.81 *0.143*	2.29 *0.116*	2.81 *0.143*	2.99 *0.151*	2.39 *0.121*	2.29 *0.115*
18–19 Feb 2000	3.42 *0.129*	3.43 *0.130*	3.35 *0.127*	3.32 *0.132*	3.13 *0.124*	3.16 *0.125*	3.51 *0.141*	3.15 *0.127*	2.72 *0.110*	3.32 *0.141*	2.97 *0.126*	2.58 *0.110*
	Wind speed (m s^{-1})											
	Alto (S1)			Bonfoi (S2)			Goedehoop (S3)			Jacobsdal (S4)		
Events	Run 1 (G2)	Run 2 (G3)	Run 3 (G4)	Run 1 (G2)	Run 2 (G3)	Run 3 (G4)	Run 1 (G2)	Run 2 (G3)	Run 3 (G4)	Run 1 (G2)	Run 2 (G3)	Run 3 (G4)
3–4 Feb 2000	2.33 *1.280*	2.07 *1.136*	0.60 *0.330*	1.28 *0.417*	1.10 *0.358*	0.95 *0.310*	1.83 *0.553*	1.48 *0.445*	1.15 *0.346*	1.14 *0.369*	1.35 *0.435*	1.32 *0.425*
12–13 Feb 2000	3.15 *0.988*	2.95 *0.925*	1.92 *0.60*	1.94 *0.434*	2.12 *0.473*	2.11 *0.471*	2.13 *0.420*	1.90 *0.374*	1.53 *0.302*	1.51 *0.320*	1.24 *0.263*	1.44 *0.305*
18–19 Feb 2000	2.38 *1.407*	2.65 *1.562*	1.62 *0.95*	1.07 *0.400*	1.60 *0.600*	1.04 *0.385*	1.40 *0.455*	1.92 *0.623*	1.56 *0.506*	1.22 *0.450*	1.23 *0.452*	1.07 *0.393*
	Relative humidity (%)											
	Alto (S1)			Bonfoi (S2)			Goedehoop (S3)			Jacobsdal (S4)		
Events	Run 1 (G2)	Run 2 (G3)	Run 3 (G4)	Run 1 (G2)	Run 2 (G3)	Run 3 (G4)	Run 1 (G2)	Run 2 (G3)	Run 3 (G4)	Run 1 (G2)	Run 2 (G3)	Run 3 (G4)
3–4 Feb 2000	10.22 *0.140*	10.30 *0.141*	9.58 *0.131*	18.21 *0.220*	10.91 *0.131*	12.94 *0.156*	15.12 *0.192*	11.80 *0.150*	9.98 *0.127*	8.68 *0.111*	5.34 *0.068*	5.46 *0.070*
12–13 Feb 2000	5.45 *0.080*	6.70 *0.099*	8.26 *0.122*	15.62 *0.195*	9.16 *0.114*	11.14 *0.134*	13.05 *0.170*	8.66 *0.112*	5.72 *0.074*	6.22 *0.086*	5.95 *0.083*	5.80 *0.080*
18–19 Feb 2000	15.06 *0.227*	10.87 *0.164*	14.12 *0.213*	23.85 *0.307*	20.12 *0.259*	22.14 *0.285*	16.83 *0.243*	15.33 *0.221*	16.30 *0.235*	17.01 *0.235*	14.87 *0.205*	13.33 *0.184*

the observations. The RMSE takes the squared weight of each $(P_i - O_i)$ into account. RMSE is among the best of the overall measures of model performance, because it summarizes the mean difference in the units of O and P (Wilmott 1982). Here, RE is a dimensionless number. RMSE can be generally regarded as a good estimate of the average error and RE as a relative difference measure.

a. Coarse resolution (grid 2, 5 km): Run 1

The deviations between observed and simulated values for the three studied meteorological variables (temperature, wind speed, and relative humidity) were generally higher using the results of the 5-km coarse resolution (run 1) than those of the other runs. For temperature, the RMSE value ranged between 1.21°C (at Bonfoi) and 4.26°C (at Goedehoop) on the first 2-day event and the RE between 5.6% and 20.2%. For wind speed, RMSE was between 1.07 m s^{-1} (at Bonfoi on 12–13 February) and 3.15 m s^{-1} (at S1, Alto, on 18–19 February) and the RE was between 32% and 140.7% (a large value), respectively. For relative humidity, RMSE was between 5.45% (at Alto on 12–13 February) and 23.85% (at Bonfoi on 18–19 February), corresponding to RE values of between 8.0% and 307%. It can be noted that the RMSE and RE values were the lowest for the two stations—S2 (Bonfoi) and S4 (Jacobsdal)—located at the center of the domain of grid 4. These two stations, therefore, are well described by the simulations of run 1 using two nested grids and a coarse resolution.

b. Fine resolution (grid 3, 1 km): Run 2

Generally, the RMSE and RE values resulting from run 2 using the 1-km fine resolution and three nested grids (grid 3) were intermediate between those of run 1 (grid 2) and run 3 (grid 4). They were either similar to those resulting from run 3 using the 200-m high resolution (grid 4) or sometimes better. For temperature, the RMSE value ranged between 1.43°C (at Jacobsdal, for the first 2-day event) and 3.43°C (at Alto, for the third 2-day event), and the relative error was between 7.0% and 13.8%. For wind speed, the RMSE was between 1.10 m s^{-1} (at Bonfoi, for the first 2-day event) and 2.95 m s^{-1} (at Alto, for the second 2-day event), and the RE was between 26.3% and 156.2%. For relative humidity, the RMSE was between 5.34% (at Jacobsdal, for the first 2-day event) and 20.12% (at Bonfoi, for the third 2-day event) associated with RE values of 6.8%–25.9%.

c. High resolution (grid 4, 200 m): Run 3

The RMSE and RE values resulting from the 200-m high resolution (run 3) and four nested grids (grid 4) were generally the best (i.e., lower values than those resulting from runs 1 and 2). For temperature, the RMSE value ranged between 1.13°C (at Bonfoi on 3–4 February) and 3.35°C (at Alto on 18–19 February) and the relative error was between 5.7% and 14.3%. For wind speed, the RMSE was between 0.60 m s^{-1} (at Alto on 3–4 February) and 2.11 m s^{-1} (at Bonfoi on 12–13 February) and the RE values were between 30.2% and 95%. For relative humidity, RMSE was between 5.46% (at Bonfoi for 18–19 February) and 22.1% (at Jacobsdal on 3–4 February) associated with RE values between 7.0% and 28.5%.

The RMSE and RE values for runs 2 and 3 were relatively similar and it was difficult to pronounce in favor of grid 4. It can, however, be concluded that the fine and high resolutions were better than the coarse resolution.

5. Diurnal variation and extreme values of main meteorological variables for the three episodes

The diurnal variations in temperature, wind speed, and relative humidity (Figs. 3–5) at each station and for each event were examined in order to study the contribution of the high-resolution grid (grid 4). Furthermore, in view of viticultural applications, it was interesting to examine the extreme values for these three variables. In Table 4, the difference between the observed and modeled maxima (Omax – Pmax) of temperature and wind speed, and the difference between the observed and modeled minima (Omin – Pmin) of relative humidity during the three studied events in the four stations are displayed. The times, at which Omax, Pmax, Omin, and Pmin occurred, were not necessarily the same. The aim of this calculation was to see if the model was able to reproduce the extreme values observed during the day.

Using the results of run 3 (with the four nested grids), this model most correctly reflected the variations in temperature, wind speed, and relative humidity compared to the simulations of the 3–4 February event (Fig. 3). Modeled data were close to the observed data and it can be noted that generally the lowest values of mean relative error were obtained at each station for this first event (Table 3) in comparison with the other 2-day events. The values were around 5%–9% for temperature, 30%–40% for wind speed, and 7%–15% for relative humidity. The most important differences between the modeled and observed results were found for Alto, located at the edge of the simulation domain. The differences between the observed and modeled maximum temperatures from run 3 (Table 4) were the lowest of the different runs except at Alto where the maximum

TABLE 4. Temperature and wind speed Omax – Pmax differences, and relative humidity Omin – Pmin difference during three studied events at four weather stations located in the Stellenbosch wine of origin district.

	Temperature (°C)							
	Alto (S1)		Bonfoi (S2)		Goedehoop (S3)		Jacobsdal (S4)	
Events	Run 2 (G3)	Run 3 (G4)	Run 2 (G3)	Run 3 (G4)	Run 2 (G3)	Run 3 (G4)	Run 2 (G3)	Run 3 (G4)
3 Feb 2000	−1.25	2.55	2.06	1.57	−2.53	2.07	2.12	2.02
4 Feb 2000	−3.12	1.08	1.56	0.76	−5.52	−1.32	0.58	0.48
12 Feb 2000	−2.71	1.99	−3.67	1.43	−5.15	−0.65	−4.98	−3.38
13 Feb 2000	1.14	4.34	−0.68	4.67	−1.57	2.93	−2.26	−2.36
18 Feb 2000	−3.4	0.24	1.27	2.24	−4.15	0.05	2.43	1.63
19 Feb 2000	2.08	0.01	−0.13	−0.03	−0.55	−1.85	−0.14	0.56
	Wind speed (m s^{-1})							
	Alto (S1)		Bonfoi (S2)		Goedehoop (S3)		Jacobsdal (S4)	
Events	Run 2 (G3)	Run 3 (G4)	Run 2 (G3)	Run 3 (G4)	Run 2 (G3)	Run 3 (G4)	Run 2 (G3)	Run 3 (G4)
3 Feb 2000	−3.99	−1.11	−2.19	−0.77	−1.96	−0.17	−1.73	−0.87
4 Feb 2000	−3.25	−0.07	−0.93	0.49	−1.39	−0.04	−0.69	−0.72
12 Feb 2000	−1.73	−0.54	−0.81	1.03	−0.85	0.65	−0.44	0.76
13 Feb 2000	−4.25	−0.61	−1.4	0.73	−2.55	−0.91	−0.63	−0.3
18 Feb 2000	−1.26	−0.23	−0.48	−1.65	0.6	1.94	−0.31	0.26
19 Feb 2000	−4.18	−2.57	−1.84	−0.32	−1.59	0.52	−1.22	0.2
	Relative humidity (%)							
	Alto (S1)		Bonfoi (S2)		Goedehoop (S3)		Jacobsdal (S4)	
Events	Run 2 (G3)	Run 3 (G4)	Run 2 (G3)	Run 3 (G4)	Run 2 (G3)	Run 3 (G4)	Run 2 (G3)	Run 3 (G4)
3 Feb 2000	−5.2	−8.2	11.4	14.8	2.6	2.0	−4.9	−3.7
4 Feb 2000	−0.8	−5.5	14.1	17.2	12.6	10.0	4.1	5.6
12 Feb 2000	−0.8	−1.9	12.2	14.3	10.4	5.2	2.6	0.6
13 Feb 2000	−14.6	−12.4	7.4	4.7	5.7	0.2	−7.3	−9.2
18 Feb 2000	6.3	4.7	20.5	21.3	8.6	7.5	7.0	9.0
19 Feb 2000	4.7	8.0	13.7	24.1	12.1	16.0	4.6	−0.3

temperature of 32°C recorded on 3 February 2000 was underestimated by the model (29.6°C) (Fig. 3a). The simulated wind speed was well estimated on average for this event at all stations. We noted at Alto a maximum wind speed of 2.82 m s^{-1} at 1600 SAST, which was overestimated (3.93 m s^{-1}) on 3 February, whereas it was well reproduced for 4 February (Fig. 3b). The largest differences were noted at Jacobsdal, the station nearest to the sea. The model seems to have underestimated the land breeze at night and overestimated the sea breeze during daytime (Fig. 3b). Furthermore, the difference between the wind speed maxima was very small for all stations (Table 4). During this episode (3–4 February), the relative humidity was sufficiently well simulated, except for Bonfoi, a station where the differences in minima were the highest (11%–17%; Table 4).

For the 12–13 February simulations, the situation with a strong southerly flow, the model reproduced the time variations of temperature and humidity well (Fig. 4). Although the maximum wind speed was well simulated (small values in Table 4), the time variation of the wind speed was not (Fig. 4). The mean relative error values for temperature were around 10%–15%, around 30%–60% for wind speed, and around 8%–13% for relative humidity (Table 3). The largest difference was found for temperature from run 3 at Jacobsdal on 12 February (Table 4).

For the event with a hot northerly flow on 18 February, followed by a weak southerly flow, the temperature, wind speed, and humidity variations were well reproduced (Fig. 5). The mean relative error values for temperature were around 11%–13%, for wind speed, they were around 38%–95%, and for relative humidity, they were around 18%–28% (Table 3). Although the air mass was hot, the differences in maximum temperatures from run 3 were low except at Bonfoi. The observed wind speed at Alto (right edge of grid 4) on 19 February was very low relative to the other stations and was not observed in the simulations. The difference between the maximum wind speeds was −2.57 at Alto, the highest for this episode. During this event, the air mass was very dry and the difference between the relative humidity minima was generally low except at Bonfoi, where the values were larger than 20%.

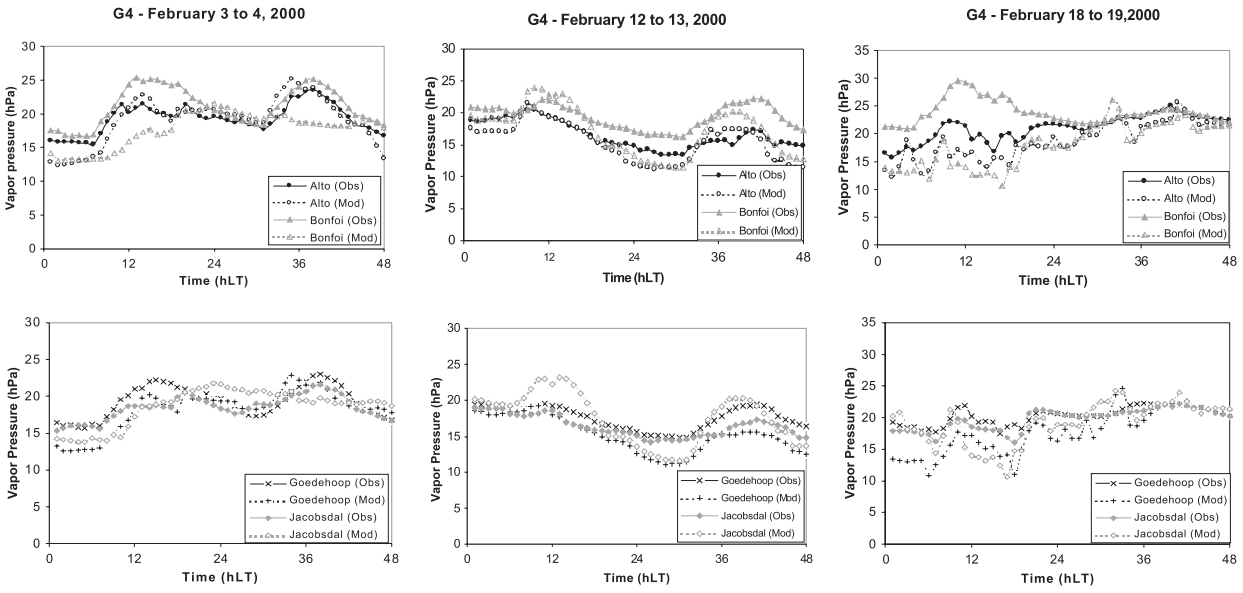

FIG. 6. Observed (solid lines) and modeled (dotted lines) data of vapor pressure at 2 m AGL for three studied events. Modeled data are extracted from run 3 using four grids.

In general, the observations from Alto, located at the right edge of grid 4 (Fig. 2c), were not properly reproduced by the model. Observations for the stations of Bonfoi and Jacobsdal, both located in the middle of the domain, were better replicated by the model results.

6. Vapor pressure and passage of the sea breeze

As the sea breeze penetrates inland, it brings moisture inland, which may be of benefit for grapevine physiology. Vapor pressure is a relevant indicator of the passage of the sea-breeze front (Helmis et al. 1987). It is calculated from temperature and relative humidity. We recall that temperature is better simulated by the model than relative humidity (sections 4 and 5). The vapor pressure calculated from run 3 is shown in Fig. 6, for the three studied events and at each station. For the two events characterized by the presence of the sea breeze (3–4 and 12–13 February 2000), both curves display a maximum occurring between 1200 and 1500 SAST, and an increase in vapor pressure at around 0900 and 1000 SAST, in agreement with the observations.

Moreover, the modeled values are close to the observed values (less than 10% difference in relative error), except for an underestimation at Bonfoi, on 3–4 February 2000, and an overestimation at Jacobsdal, on 12–13 February 2000. For the third event (18–19 February 2000), with no sea-breeze occurrence, on 18 February the numerical results are underestimated versus the observations particularly at Bonfoi. In this case, the form of the curves is very different from previous events. Figure 7 displays the vapor pressure, similarly to Fig. 6, but for grid 3 derived from run 2. To examine the contribution from a high-resolution mode such as grid 4, we compared Figs. 6 and 7. In both figures, the forms of the curves are similar, but the maximum values were often different. For instance, vapor pressure was overestimated at Alto (30 instead of 25 hPa) and at Goedehoop (27 instead of 24 hPa) on 4 February (Fig. 7), and at Alto (24 instead of 20 hPa) on 12 February. These overestimations do not exist in Fig. 6. In general, vapor pressure was better simulated using the high resolution of run 3 than using the low resolution of run 2. It is an important result that favors the use of high resolution.

The sea-breeze passage is characterized by the increase in vapor pressure and the change in wind direction simultaneously. The observed wind direction and the wind direction calculated from run 3 for the three studied events and in each station are shown in Fig. 8. For the events of 3–4 and 12–13 February 2000, a sea-breeze circulation occurred during the afternoon for the 2 days, with southerly to southwesterly winds (i.e., 180°–270°). At night the wind direction was reversed. The calculated wind direction for these two events is in agreement with the observations. However, we noted that the observed night extreme values indicating a northerly direction (inferior to 50° or superior to 300°) were not often reached by the modeled values. Nevertheless, if we compare Figs. 6 and 8, we can see, in both observed and modeled data, that the change in wind direction was correlated to the increase in vapor pressure at

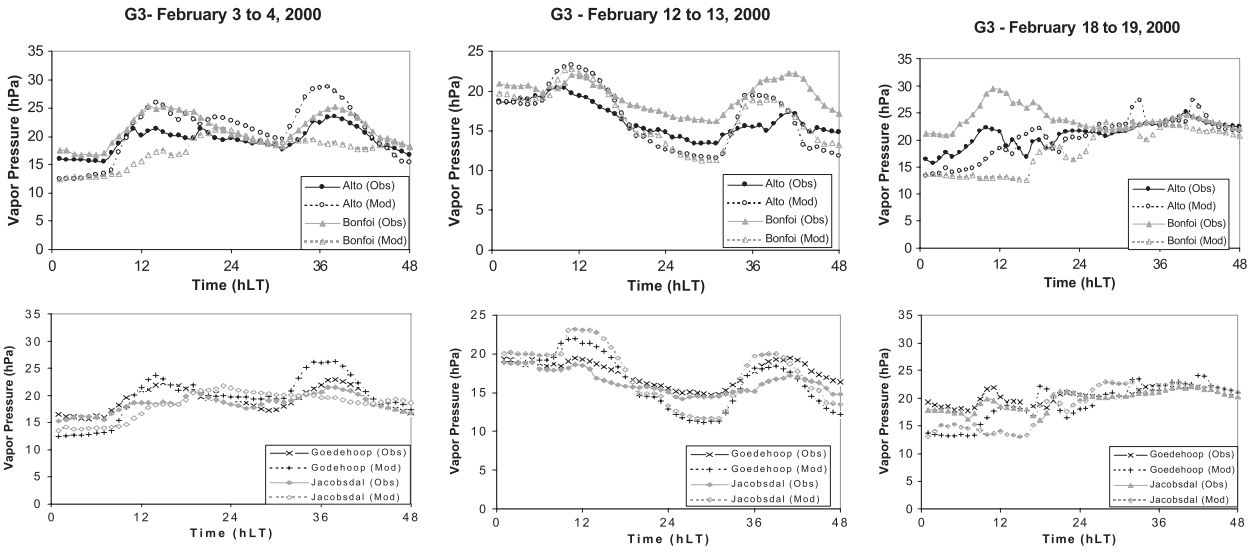

FIG. 7. As in Fig. 6, but with data extracted from run 2 using three grids.

around 0900–1000 SAST, and that the maximum values of vapor pressure at around 1200–1500 SAST was associated with a southerly to southwesterly wind (sea breeze). For the event of 18–19 February 2000, the southerly to southwesterly wind direction prevailed on the last day (19) only, at all stations except at Alto. In this event, the numerical results were in agreement with the observations too. Generally, the timing of the sea-breeze frontal movement was well reproduced in this region by the model.

7. Modeled mean temperature, wind speed, and relative humidity for February 2000

The mean hourly temperature, relative humidity, and wind speed for the month of February 2000 (mean results for the 29 days) were computed. The mean temperature, wind speed, and relative humidity are displayed in Figs. 9–11 , respectively, for grid 3 (the a panels) and grid 4 (the b panels) at 1400 SAST, a time at which the temperature reached its maximum, and mean

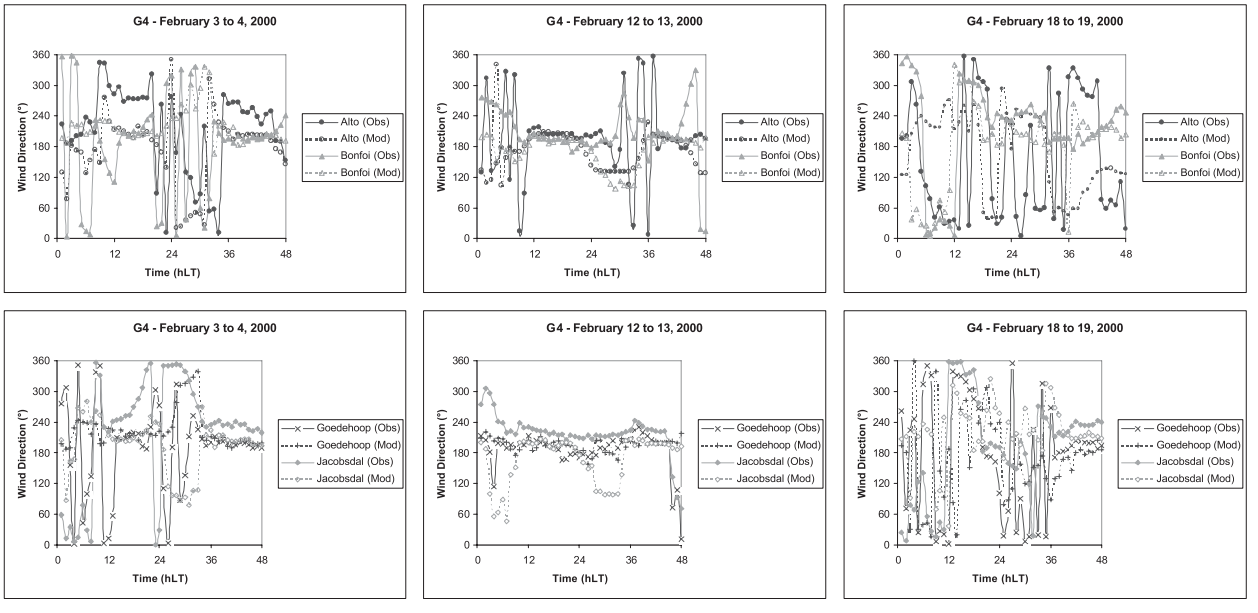

FIG. 8. Observed (solid lines) and modeled (dotted lines) wind direction at 2 m AGL for three studied events. Modeled data are extracted from run 3 using four grids.

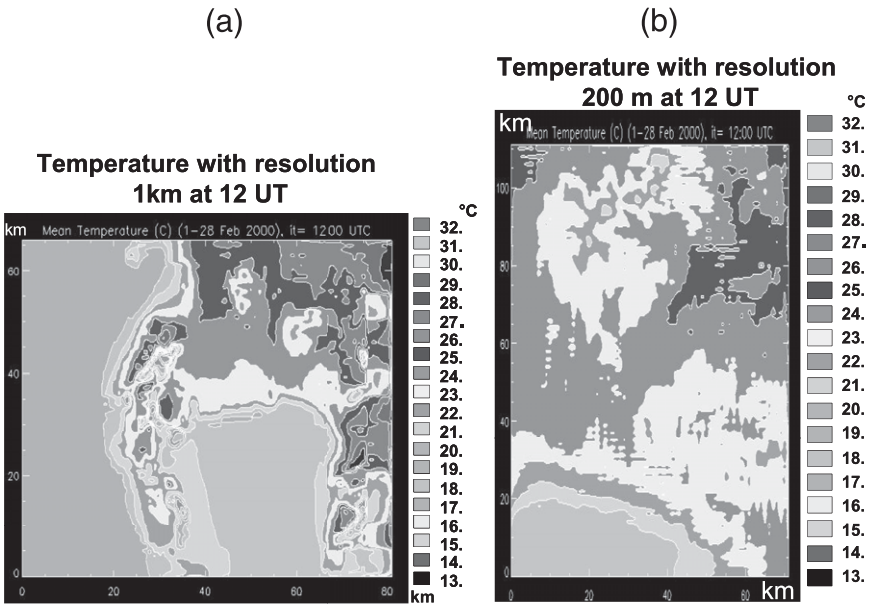

FIG. 9. Mean February 2000 temperature at 1400 SAST for (a) grid 3 (1-km resolution) and (b) grid 4 (200-m resolution).

radiation is displayed in Figs. 12a and 12b for grid 3 and grid 4, respectively, at 1300 SAST, a time at which the radiation reached its maximum. Taking grid 3 into consideration (Fig. 9a), the optimum temperature requirements for grapevine photosynthesis (25°–30°C) were met in the region located approximately 5 km from Table Bay and 10 km from False Bay, corresponding to the bottom northwestern slopes of the Helderberg and Bottelaryberg hills within grid 4 (Fig. 9b). Similarly, the optimum relative humidity requirements (60%–70%) were met near the coast up to 5 km inland from Table Bay and up to 15 km inland from False Bay (Fig. 10a), that is, including the southern part of Stellenbosch. The modeled monthly means are smoothed compared to the observed monthly means (Table 5) but the main features of the sea breeze are well distinguished. The wind speed (Fig. 11) is generally 9–10 m s^{-1} at the coastline. The lowest velocities (5–6 m s^{-1}) immediately adjacent to the

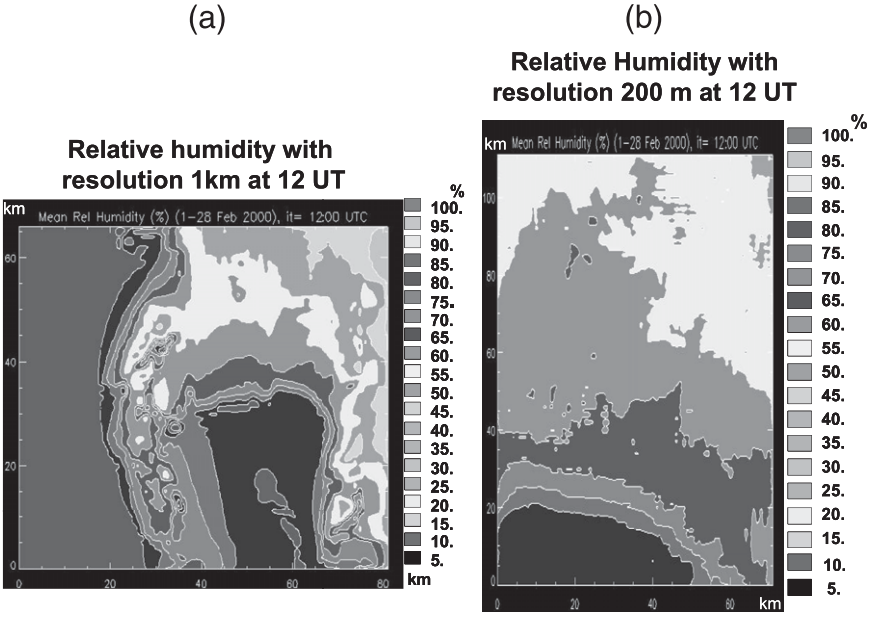

FIG. 10. As in Fig. 9, but for relative humidity.

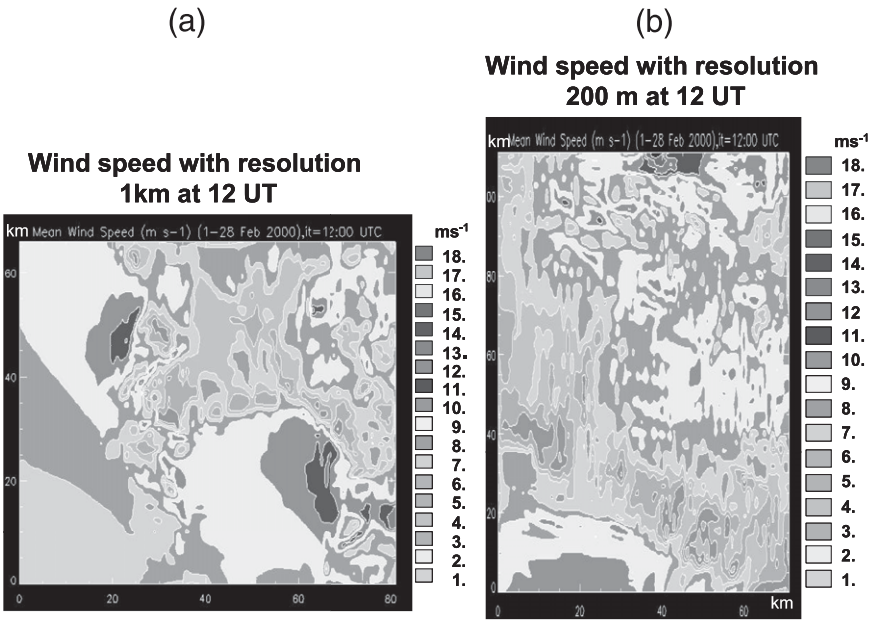

FIG. 11. As in Fig. 9, but for wind speed.

coastline (Fig. 11b) are due to the sudden roughness of the land surface generated by dune ridges 80 m high, parallel to the coast and covered by evergreen shrubs, as was already shown by Bonnardot et al. (2001). The maximum velocity inland was of 10 m s^{-1} on the southern slope of the Bottelaryberg hills, that is, above the 4 m s^{-1} threshold, which inhibits photosynthesis (Bonnardot et al. 2001).

Most of the region included within grid 4 had a maximum radiation of 950 W m^{-2}, reaching 1000 W m^{-2} in the top-right corner of grid 4, with variations of up to 100 W m^{-2} at any point. One can clearly see the supplementary information given by the high resolution (Fig. 12b) compared to the 1-km resolution (Fig. 12a) due to various slopes and aspects and distance from the coast. The most important differences between grids 3 and 4

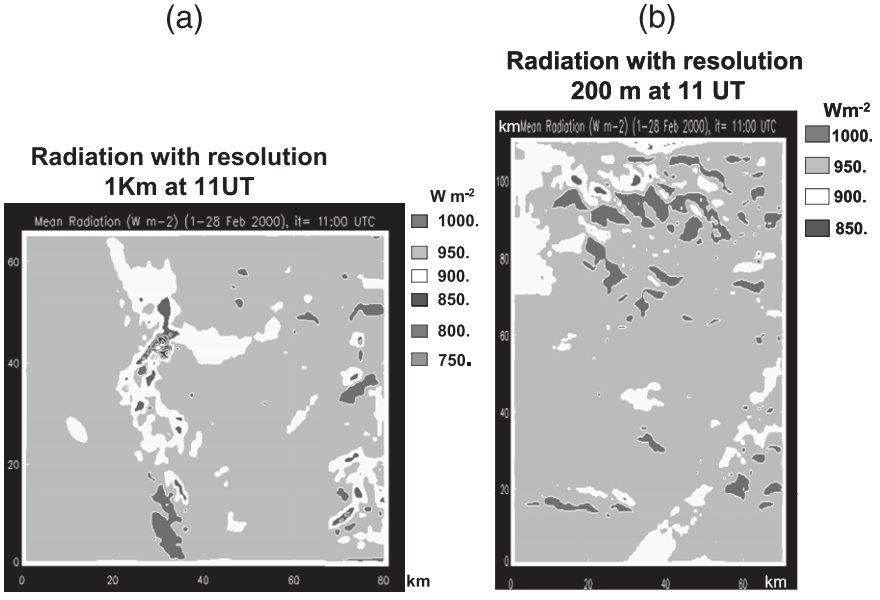

FIG. 12. Mean February 2000 radiation at 1300 SAST for (a) grid 3 (1-km resolution) and (b) grid 4 (200-m resolution).

TABLE 5. Hourly mean temperature (temp), wind speed (wind), and relative humidity (RH) at four weather stations located in the Stellenbosch wine of origin district (February 2000).

Stations	Alto (S1)			Bonfoi (S2)			Goedehoop (S3)			Jacobsdal (S4)		
Time (SAST)	Temp (°C)	Wind (m s^{-1})	RH (%)	Temp (°C)	Wind (m s^{-1})	RH (%)	Temp (°C)	Wind (m s^{-1})	RH (%)	Temp (°C)	Wind (m s^{-1})	RH (%)
0100	19.23	1.49	80.89	18.79	2.17	87.19	18.27	2.70	83.56	17.60	2.42	84.17
0200	18.98	1.31	81.54	18.35	2.03	88.44	17.97	2.39	84.47	17.41	2.37	84.78
0300	18.78	1.31	81.63	18.06	2.1	89.19	17.79	2.38	84.93	17.34	2.40	85.00
0400	18.47	1.24	82.42	17.93	2.05	89.51	17.60	2.34	85.38	17.18	2.40	85.89
0500	18.44	1.18	82.73	17.93	2.03	89.23	17.48	2.49	85.63	17.10	2.40	86.42
0600	18.32	1.19	83.06	17.90	1.85	89.29	17.36	2.44	85.97	16.91	2.18	86.64
0700	18.26	1.11	82.99	17.89	1.79	89.27	17.45	2.43	85.18	17.10	2.10	85.96
0800	19.37	1.10	82.41	19.56	1.96	85.51	18.60	2.30	82.18	18.66	2.26	80.87
0900	21.20	1.33	78.69	21.46	2.47	80.11	20.32	2.66	77.11	20.74	2.71	73.30
1000	23.18	1.73	73.21	23.53	3.15	73.47	22.30	3.07	70.87	22.71	3.21	65.78
1100	25.45	2.14	66.83	25.28	3.67	68.90	24.18	3.67	66.53	24.23	3.69	60.83
1200	27.18	2.47	62.12	26.41	4.17	66.13	25.40	4.14	62.63	25.23	4.20	57.73
1300	28.54	2.70	59.70	27.07	4.54	64.87	26.06	4.55	61.05	25.70	4.59	56.79
1400	29.20	3.01	58.61	27.33	5.16	64.46	26.34	5.01	60.94	26.07	4.82	55.98
1500	29.37	3.16	58.22	27.40	5.51	64.18	26.30	5.49	61.27	26.02	5.09	56.16
1600	29.19	3.27	58.36	26.98	5.87	64.84	25.95	5.90	62.16	25.65	5.27	57.45
1700	28.66	3.28	59.18	26.34	5.76	66.57	25.25	6.08	63.94	24.01	5.24	59.47
1800	27.68	3.17	60.59	25.49	5.51	68.51	24.31	6.15	66.24	24.28	4.91	61.74
1900	26.11	2.86	63.13	24.12	4.75	72.92	23.07	5.55	70.12	22.88	4.54	67.27
2000	23.67	2.45	69.27	22.06	3.83	79.14	21.15	4.86	75.82	20.73	3.80	75.31
2100	21.79	2.02	75.10	20.82	3.22	82.83	19.83	4.08	80.33	19.46	3.12	79.77
2200	20.69	1.74	78.38	20.22	2.97	84.32	19.23	3.73	82.33	18.82	2.77	81.72
2300	20.10	1.70	79.96	19.68	2.70	85.82	18.83	3.34	83.46	18.34	2.66	83.04
0000	19.67	1.51	80.43	19.22	2.29	86.88	18.59	3.00	83.66	18.04	2.58	83.61

were found in radiation (and wind speed), probably due the nonlinear relationship with a heterogeneous surface.

The hourly means for February 2000 and for the four stations are displayed in Fig. 13 and Table 5. The observed mean temperature, wind speed, and relative humidity are compared to the modeled mean temperature, wind speed, and relative humidity obtained from run 3. The curves of temperature were in good agreement for all stations except for the high values during the day at Alto. Alto had a different pattern of behavior with respect to the curves for wind speed compared to the observed data at other stations, which was also not taken into account by the model. The differences between the observed and modeled values for each hour are around 1–1.5 m s^{-1}. For the other stations, the model displayed the same pattern as the observations. The maximum for each station was, however, slightly overestimated (around 0.5 m s^{-1}). The curves for relative humidity showed accurately high values at night and lower values during the day. The low values were in good agreement with the observations for Alto and Jacobsdal. Humidity was, however, underestimated for Bonfoi and Goedehoop during the middle of the day. Similarly to section 6, it can be concluded in general that the observations and numerical results were in good agreement except for the station of Alto located at the eastern margin of grid 4.

8. Discussion and conclusions

As a whole, the observed differences in temperature and relative humidity between the four stations were reduced during the events with a strong synoptic flow (12 and 18–19 February), whereas differences between stations were noted for the days where local air circulations were controlled by sea and slope breezes (3–4 and 13 February). For each event, it was noted that the wind speeds and direction recorded at Alto were not associated with those recorded at the other stations (due to differences in aspect, in that it did not face the sea).

Was the RAMS model able to replicate these observations for local sea-breeze circulations? Run 3 with grid 4 showed accurate numerical results for the first event (Table 3), with the lowest relative errors: 5%–9% for temperature, 30%–40% for wind speed, and 7%–15% for relative humidity. With run 2 and grid 3 the relative errors were 7%–13.8% for temperature, 35%–113% for wind speed, and 7%–15% for relative humidity. For this first event (weak synoptic flow and sea breeze bringing humidity inland), the differences between the

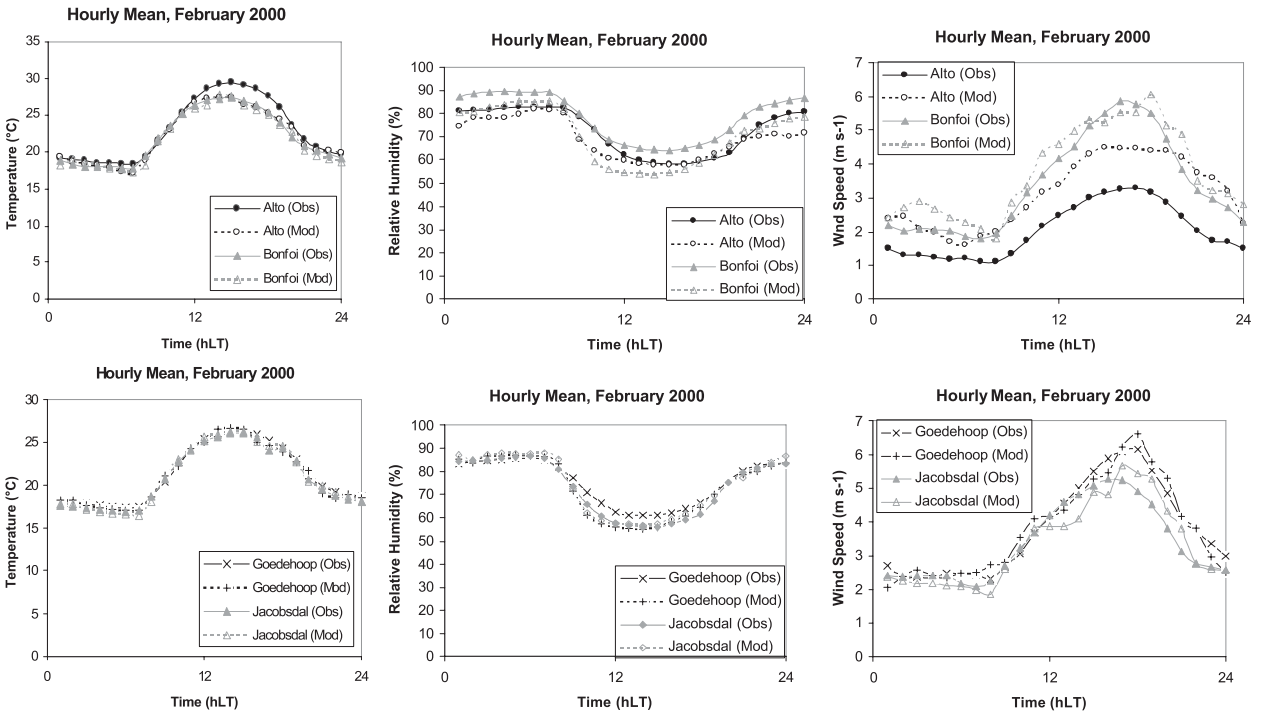

FIG. 13. Observed (solid lines) and modeled (dotted lines) hourly means for temperature, wind speed, and relative humidity at 2 m AGL during February 2000. Modeled data are extracted from run 3 using four grids.

observed and modeled extreme values for temperature and relative humidity (Table 4) had the same order of magnitude in runs 3 and 2, whereas for wind speed run 3 gave more accurate results than run 2. Furthermore, the vapor pressure derived from run 3 was closer to the observed data than the one derived from run 2. Although it was noticed that run 3 gave more accurate results than run 2 (also depending on how RAMS was set up), the study was based on simulations for three events only and, thus, is not necessarily representative of all aspects of the different synoptic conditions over the cape.

In cases with a prevailing synoptic flow (12–13 and 18–19 February), run 2 with grid 3 was generally as accurate as run 3 with grid 4. The relative errors between the modeled and observed values were 11%–14% for temperature and 8%–28% for relative humidity. However, RAMS seemed to have difficulties in simulating comparable wind speeds when the observed wind speeds were low (the relative errors for wind speed were between 26% and 156%).

For each event, fine- and high-resolution (1 km and 200 m, respectively) simulations displayed improvements relative to the 5-km-resolution simulation, especially in reproducing the local air circulations (sea and slope breezes) because of a better representation of the local terrain (topography, vegetation cover). This was also shown by Zhang et al. (2005) and Gego et al. (2005).

With a strong synoptic flow, the increasing horizontal resolution of the grid did not necessarily give more information, and the results of the 1-km-resolution simulation often seemed sufficient to describe the different local air circulations. On the other hand, with a weak synoptic flow and prevailing local air circulations, as often occurs during the month of February, the high horizontal resolution (200 m) displayed relevant meteorological information for viticultural applications.

Furthermore, with the high resolution (200 m), we showed that the increase in vapor pressure in the morning was associated with the change in wind direction as the sea breeze occurred and that the maximum values of vapor pressure at around 1200–1500 SAST were associated with a southerly to southwesterly wind (sea breeze), just as for the observations and for all stations. Generally, the timing of the sea-breeze frontal movement was well retrieved in this region by the model.

Moreover, in view of viticultural applications, the model correctly reproduced the extreme values of temperature (those exceeding 30°C), wind speed (those exceeding 5 m s^{-1}), and relative humidity (those below 60%). In the three events that were examined, measurements showed that the temperature threshold of 30°C for photosynthesis was exceeded on 3 February at Alto and on 18 February for all stations. The model

gave a value of 30.1°C at 1300 SAST at Alto and indicated accurate values for 18 February for all stations. In the case of the wind, the value of 8 m s^{-1} was exceeded on 12–13 February and the model accurately reproduced it. In view of these case studies, the model had difficulties in reproducing the low wind speed values, which, indeed, does not diminish its application in viticultural studies. For each event, relative humidity was below 60% and the model accurately reproduced this value on each occasion. Considering the results of the study, the following main conclusions can be drawn:

- Local air circulations, such as sea or slope breezes, were better described using fine and high resolutions (1 km and 200 m, respectively, in the horizontal dimension) than with a coarse 5-km resolution.
- Considering the main meteorological variables (especially the different thresholds for viticulture), the results from the fine 1-km resolution (run 2) were as accurate as the results from the high 200-m resolution (run 3), except for the first event when an ''intense'' sea-breeze circulation developed over the study area.
- Results for locations situated at the center of grids (simulation domains) were correctly reproduced by the model.
- When used at fine and high resolutions, as presented here, RAMS can be used for viticultural and other agricultural purposes.

Acknowledgments. Measurements from the different stations were provided by the Institute for Soil, Climate and Water of the Agricultural Research Council (ARC-ISCW). Thanks are given to the Wine Industry Network of Expertise and Technology (WINETECH), which partly funded this project. This modeling study is supported by funding from the French Centre National de la Recherche Scientifique (Programme National de Chimie Atmosphérique). Computer resources were provided by Centre Informatique National de l'Enseignement Supérieur (CINES) Project AMP2107. The authors also thank the computer team of the Laboratoire de Météorologie Physique of the Blaise Pascal—A. M. Lanquette, S. Banson, and Ph. Cacault—and, finally, the reviewers for their pertinent comments and input, which contributed to improvements in the final version of this paper.

REFERENCES

Abbs, D. J., and W. L. Physick, 1992: Sea breeze observations and modelling: A review. *Aust. Meteor. Mag.,* **41,** 7–19.

Bonnardot, V., 1999: Étude préliminaire des brises de mer pendant la période de maturation dans la région viticole du Cap en Afrique du Sud. *Pub. Assoc. Int. Climatol.,* **12,** 26–33.

——, 2002: The sea breeze: a significant climatic factor for viticultural zoning in coastal wine producing areas. *Proc. IVth Int. Symp. on Viticultural Zoning*, Vol. 1, Avignon, France, Syndicat Professionnel Inter Rhône, 339–348.

——, V. A. Carey, O. Planchon, and S. Cautenet, 2001: Sea breeze mechanism and observations of its effects in the Stellenbosch wine producing area. *Wynboer,* **147,** 10–14.

——, O. Planchon, V. A. Carey, and S. Cautenet, 2002: Diurnal wind, relative humidity and temperature variation in the Stellenbosch-Groot Drakenstein wine producing area. *S. Afr. J. Enol. Vitic.,* **23,** 62–71.

——, ——, and S. Cautenet, 2005: The sea breeze development under an offshore synoptic wind in the South Western Cape and implications over the Stellenbosch wine-producing area. *Theor. Appl. Climatol.,* **81,** 203–218.

Campbell-Clause, J. M., 1988: Stomatal response of grapevines to wind. *Aust. J. Exp. Agric.,* **38,** 77–82.

Carey, V. A., 2001: Spatial characterization of terrain units in the Bottelaryberg/Simonsberg/Helderberg winegrowing area. M.S., Agriculture, Department of Viticulture, University of Stellenbosch, Matieland, South Africa, 90 pp.

——, E. Archer, and D. Saayman, 2002: Natural terroir units: What are they? How can they help the wine farmer? *Wynboer,* **151,** 86–88.

Champagnol, F., 1984: *Eléments de Physiologie de la Vigne et de Viticulture Générale*. Saint-Gely-du-Fesc, 351 pp.

Chen, F., R. Pielke Sr., and K. Mitchell, 2001: Development and application of land-surface models for mesoscale atmospheric models: Problems and promises. *Observation and Modeling of the Land Surface Hydrological Processes,* V. Lakshmi, J. Albertson, and J. Schaake, Eds., Amer. Geophys. Union, 107–135.

Clark, T. L., and R. D. Farley, 1984: Severe downslope windstorm calculations in two and three spatial dimensions using an elastic interactive grid nesting: A possible mechanism for gustiness. *J. Atmos. Sci.,* **41,** 329–350.

Colby, F. P., Jr., 2004: Simulation of the New England sea breeze: The effect of grid spacing. *Wea. Forecasting,* **19,** 277–285.

Conradie, W. J., V. A. Carey, V. Bonnardot, D. Saayman, and L. H. Van Schoor, 2002: Effect of natural ''terroir'' units on the performance of Sauvignon blanc grapevines in the Stellenbosch/Durbanville districts of South Africa. I. Geology, soil, climate, phenology and grape composition. *S. Afr. J. Enol. Vitic.,* **23,** 78–91.

Coombe, B. G., 1987: Influence of temperature on composition and quality of grapes. *Acta Hortic.,* **206,** 23–33.

Cotton, W. R., Sr., and Coauthors, 2003: RAMS 2001: Current status and future directions. *Meteor. Atmos. Phys.,* **82,** 5–29.

De Villiers, F. S., 1997: The use of Geographic Information System (GIS) in the selection of wine cultivars for specific areas by using temperature climatic models. *Proc. XXII Congrès de la Vigne et du Vin*, Buenos Aires, Argentina, Office International de la Vigne et du Vin, 14 pp.

——, A. Schmidt, J. C. D. Theron, and R. Taljaard, 1996: Onderverdeling van die Wes-Kaapse wynbougebiede volgens bestaande klimaatskriteria. *Wynboer,* **78,** 10–12.

Du Preez, C. B., 2006: A mesoscale investigation of the sea breeze in the Stellenbosch winegrowing district. M.S. dissertation, Dept. of Meteorology, University of Pretoria, Pretoria, South Africa, 98 pp.

Düring, H., 1976: Studies on the environmentally controlled stomatal transpiration in grape vines. I. Effects of light intensity and air humidity. *Vitis,* **15,** 82–87.

Falcetti, M., 1994: Le Terroir. Qu'est-ce qu'un terroir? Pourquoi l'étudier? Pourquoi l'enseigner? *Bull. O.I.V.,* **67,** 246–275.

Freeman, B. M., W. M. Kliewer, and P. Stern, 1982: Influence of windbreaks and climatic region on diurnal fluctuation of leaf water potential, stomatal conductance, and leaf temperature of grapevines. *Amer. J. Enol. Vitic.,* **33,** 233–236.

Gego, E., Ch. Hogrefe, G. Kallos, A. Voudouri, J. S. Irwin, and S. Trivikrama Rao, 2005: Examination of model predictions at different horizontal grid resolutions. *Environ. Fluid Mech.,* **5,** 63–85.

Gladstones, J., 1992: *Viticulture and Environment*. Winetitles, 310 pp.

Hamilton, R. P., 1989: Wind and its effects on viticulture. *Austr. Grapegr. Winemaker,* **16,** 17.

Helmis, C. G., D. N. Asimakopoulos, D. G. Deligiorgi, and D. P. Lalas, 1987: Observations of sea breeze fronts near the shoreline. *Bound.-Layer Meteor.,* **38,** 395–410.

Huglin, P., and C. Schneider, 1998: *Biologie et Écologie de la Vigne*. 2nd ed. Lavoisier, 370 pp.

Hunter, J. J., and V. Bonnardot, 2002: Climatic requirements for optimal physiological processes: A factor in viticultural zoning. *Proc. IVth Int. Symp. on Viticultural Zoning*, Avignon, France, Syndicat Professionnel Inter Rhône, 553–565.

Jackson, R. S., 2000: *Wine Science. Principles, Practice, Perception*. 2nd ed. Academic Press, 65 pp.

Kliewer, W. M., and R. E. Torres, 1972: Effect of controlled day and night temperatures on grape coloration. *Amer. J. Enol. Vitic.,* **23,** 71–77.

Kriedemann, P. E., 1968: Photosynthesis in vine leaves as a function of light intensity, temperature, and leaf age. *Vitis,* **7,** 213–220.

Land Type Survey Staff, 1995: Land types of the map 3318 CAPE TOWN. Memoirs, Agriculture and Natural Resources, South Africa, Vol. 24, Institute for Soil, Climate and Water of the Agricultural Research Council, 20 pp.

Le Roux, E. G., 1974: 'n Klimaatsindeling van die Suidwes-Kaaplandse Wynbougebiede. M.S. thesis, University of Stellenbosch, Matieland, South Africa, 103 pp.

Marais, J., 1994: Sauvignon blanc cultivar aroma—A review. *S. Afr. J. Enol. Vitic.,* **15,** 41–45.

——, J. J. Hunter, and P. D. Haasbroek, 1999: Effect of canopy microclimate season and region on Sauvignon blanc grape composition and wine quality. *S. Afr. J. Enol. Vitic.,* **20,** 19–30.

Mass, C. F., D. Ovens, K. Westrick, and B. A. Colle, 2002: Does increasing horizontal resolution produce more skillful forecasts? *Bull. Amer. Meteor. Soc.,* **83,** 407–430.

McQueen, J. T., R. R. Draxler, and G. D. Rolph, 1995: Influence of grid size and terrain resolution on wind field predictions from an operational mesoscale model. *J. Appl. Meteor.,* **34,** 2166–2181.

Miller, S. T. K., B. D. Keim, R. W. Talbot, and H. Mao, 2003: Sea breezes: Structure, forecasting and impacts. *Rev. Geophys.,* **41,** 1011, doi:10.1029/2003RG000124.

Planchon, O., V. Bonnardot, and S. Cautenet, 2000: Simulation de brise de mer dans la Province Occidentale du Cap (résolution à 5 km): Exemple de la journée du 4 février 2000. *Pub. Assoc. Int. Climatol,* **13,** 482–489.

Preston-White, R. A., and P. D. Tyson, 1988: *The Atmosphere and Weather of Southern Africa*. Oxford University Press, 386 pp.

Rao, P. A., H. E. Fuelberg, and K. K. Droegemeier, 1999: High resolution modeling of the Cape Canaveral area land–water circulations and associated features. *Mon. Wea. Rev.,* **127,** 1808–1821.

SAWIS, 2006: Annual Booklet 30. South African Wine Industry Statistics, 31 pp. [Available from SAWIS, P.O. Box 238, Paarl, 7620, South Africa.]

Schulze, B. R., 1994: *Climate of South Africa*. Part 8, *General Survey,* 1st ed., Department of Environment Affairs, Weather Bureau, Republic of South Africa, 330 pp.

Walko, R. L., C. J. Tremback, R. A. Pielke, and W. R. Cotton, 1995: An interactive nesting algorithm for stretched grids and variable nesting ratios. *J. Appl. Meteor.,* **34,** 994–999.

Willmott, C. J., 1982: Some comments on the evaluation of model performance. *Bull. Amer. Meteor. Soc.,* **63,** 1309–1313.

Zhang, Y., Y.-L. Chen, Yi-Leng, T. A. Schroeder, and K. Kodama, 2005: Numerical simulations of sea-breeze circulations over northwest Hawaii. *Wea. Forecasting,* **20,** 827–846.